ELSEVIER

Journal of Alloys and Compounds 303–304 (2000) 223–227

Journal of ALLOYS AND COMPOUNDS

www.elsevier.com/locate/jallcom

Magnetic properties of icosahedral R–Mg–Zn quasicrystals (R=Y, Tb, Dy, Ho and Er)

I.R. Fisher[a,*], Z. Islam[a], J. Zarestky[a], C. Stassis[a], M.J. Kramer[b], A.I. Goldman[a], P.C. Canfield[a]

[a] *Department of Physics and Astronomy, Ames Laboratory, Iowa State University, Ames, IA 50011, USA*

[b] *Department of Materials Science and Engineering, Ames Laboratory, Iowa State University, Ames, IA 50011, USA*

Abstract

Large (up to 0.5 cm^3) single grains of icosahedral R–Mg–Zn quasicrystals (R=Y, Tb, Dy, Ho and Er) have been grown via a self-flux technique. The samples have a composition of approximately $R_9Mg_{34}Zn_{57}$, and are extremely well-ordered, with little or no evidence of phason strain. These samples have allowed a detailed investigation of the magnetic behaviour of local 4*f* moments in a quasiperiodic environment. Neutron scattering experiments using powdered single-grains show no evidence for long range magnetic order in the R–Mg–Zn quasicrystals. However, magnetization and magnetic susceptibility measurements indicate a spin-glass state, with freezing temperatures T_f=5.8, 3.6, 2.0 and 1.3 K for R=Tb, Dy, Ho and Er respectively. Deviations from a Curie-Weiss temperature dependence of the susceptibility are small, and only occur for temperatures up to 5 K above T_f, indicating the absence of any significant cluster glass behaviour. In addition, the rare earth dilution series $(Y_{1-x}Gd_x)$–Mg–Zn have lower freezing temperatures than $(Y_{1-x}Tb_x)$–Mg–Zn, despite the larger de Gennes factor of Gd^{3+} over Tb^{3+}, indicating that crystal electric fields play a significant role in the freezing phenomenon. This difference between Heisenberg and non-Heisenberg moments is further explored via several $(Gd_{1-x}R_x)$–Mg–Zn pseudo-ternary quasicrystal series.

Keywords: Quasicrystals; Crystal growth; Magnetic measurements; Spin glass

1. Introduction

Quasicrystals are well ordered solids, with sharp diffraction peaks. By discarding the conventional requirement of translational periodicity, quasicrystals possess crystallographically forbidden rotational symmetries, such as five-fold symmetric axes [1]. The most recent example of a stable icosahedral phase in the R–Mg–Zn family (R=Y, Tb, Dy, Ho, Er) [2,3] has generated a great deal of excitement because of the opportunity for new investigations of magnetism involving localized 4*f* moments on a quasiperiodic lattice (i.e. a well-ordered lattice, but lacking translational periodicity). Initial magnetic measurements using polygrain samples (from rapidly cooled melts) indicated a spin glass state at low temperatures [4], however, there was some ambiguity as to the nature of the spin freezing transition [5]. Sharp peaks in neutron diffraction data (albeit with a very low intensity) were initially interpreted as evidence for long range magnetic order (with $T_N \approx 20$ K for Tb–Mg–Zn) [6], although not all the peaks could be indexed by one scheme (indicating magnetic second phases) and there were missing diffraction peaks compared to the theoretically allowed symmetries [7]. By growing the first large, high-purity, single-grain R–Mg–Zn quasicrystals [8], we have been able to unambiguously demonstrate the absence of long range magnetic order in this icosahedral quasicrystal via powder neutron diffraction experiments [9]. These measurements were subsequently independently confirmed by Sato et al. [10], and the general consensus is now that there is no long range magnetic order in this system (implying either the presence of magnetic second phases in the polygrain samples used for the initial powder neutron diffraction experiments of Charrier et al. [6], or a considerable width of formation of the icosahedral phase, which based on compositional analysis [11] we believe to be unlikely). Sato et al. [10] have also demonstrated the icosahedral symmetry of the short range correlations associated with the spin glass state by single-grain neutron diffraction. In addition, we have been able to carefully investigate the magnetic properties of our single-grain samples, and make definitive thermodynamic measurements that fully establish the spin glass nature of the low-temperature state [12]. Finally, by considering the two solid solutions $(Y_{1-x}Tb_x)$–Mg–Zn

*Corresponding author.

0925-8388/00/$ – see front matter
PII: S0925-8388(00)00635-6

and $(Y_{1-x}Gd_x)$–Mg–Zn we have been able to investigate the origins of the spin freezing transition, concluding that both the multiplicity of R–R distances in the quasicrystalline lattice, and also the local R environment contribute to the spin freezing phenomenon [12]. This paper summarizes the results that we have presented elsewhere for the magnetic properties of the icosahedral R–Mg–Zn quasicrystals [8,9,12], and introduces some preliminary results for the magnetic rare earth substitutions $(Tb_{1-x}R_x)$–Mg–Zn and $(Dy_{1-x}R_x)$–Mg–Zn.

2. Experimental methods

Single grain samples of icosahedral R–Mg–Zn (R=Y, Tb, Dy, Ho and Er) quasicrystals with volumes of up to 0.5 cm^3 have been grown from the ternary melt (i.e. a self flux method) [8]. In brief, this method involves the slow cooling of a ternary melt intersecting the primary solidification surface of the icosahedral phase, as identified by Langsdorf, Ritter and Assmus [13]. The samples have a dodecahedral morphology, with pentagonal facets, reflecting the face centered icosahedral symmetry of the quasicrystalline phase. A photograph of a typical R–Mg–Zn quasicrystal is shown in Fig. 1 (from Fisher et al. [12]). The flux growth technique is extremely versatile, and several other families of quasicrystals have also been successfully grown in single-grain form using these general principles (for instance, the decagonal Al–Ni–Co phase [14]).

The single-grain R–Mg–Zn quasicrystals grown via this technique are exceptionally well ordered, with correlation lengths estimated from single-grain X-ray diffraction experiments of greater than 1000 Å. Furthermore, there is no evidence from high resolution transmission electron microscopy of any phason strain in these samples (a common defect in quasicrystals) [8]. The samples have a composition of $R_9Mg_{34}Zn_{57}$.

Powder neutron diffraction experiments were performed on crushed single-grain samples of icosahedral Tb–Mg–Zn using the HB1A triple-axis diffractometer at the High Flux Isotope Reactor (HFIR) at Oak Ridge National Laboratory, as described in more detail by Islam et al. [9]. By using crushed single-grains (as opposed to powder samples obtained by rapidly cooling a stoichiometric melt) we are guaranteed high-purity samples for these experiments, free from magnetic second phases that might produce spurious sharp diffraction peaks.

Magnetic measurements were performed using a Quantum Design MPMS SQUID magnetometer, in the temperature range from 1.8 to 350 K, and in applied fields up to 55 kOe. All data were taken while warming the sample, following either an initial zero-field-cool (zfc) or field-cool (fc). Further experimental details are given in Ref. [12].

3. Results and discussion

The powder neutron diffraction data described in detail by Islam et al. [9] can be summarized by the data shown in Fig. 2. Here we show the difference intensity between 4 K ($T < T_f$) and 30 K ($T > T_f$) as a function of scattering angle (remembering that the initial claims of long range magnetic order indicated $T_N \approx 20$ K [6]). Note the absence of any sharp diffraction peaks, implying the absence of long range magnetic order in these high-purity samples. However, short range correlations associated with the low-

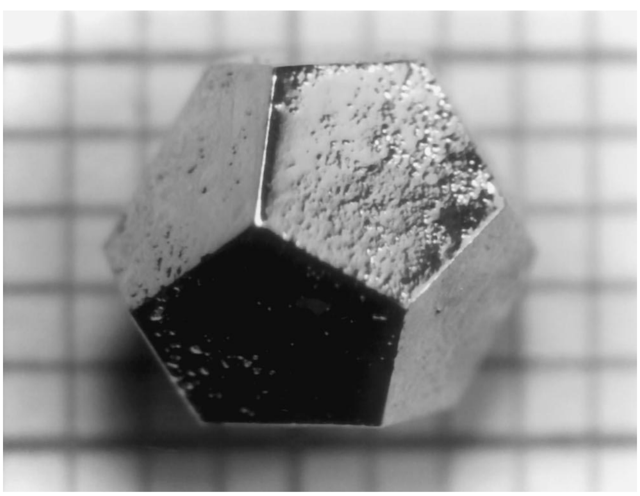

Fig. 1. Photograph of a single-grain icosahedral Ho–Mg–Zn quasicrystal, shown over a mm scale. Note the clearly defined pentagonal facets and the dodecahedral morphology. From Fisher et al. [12].

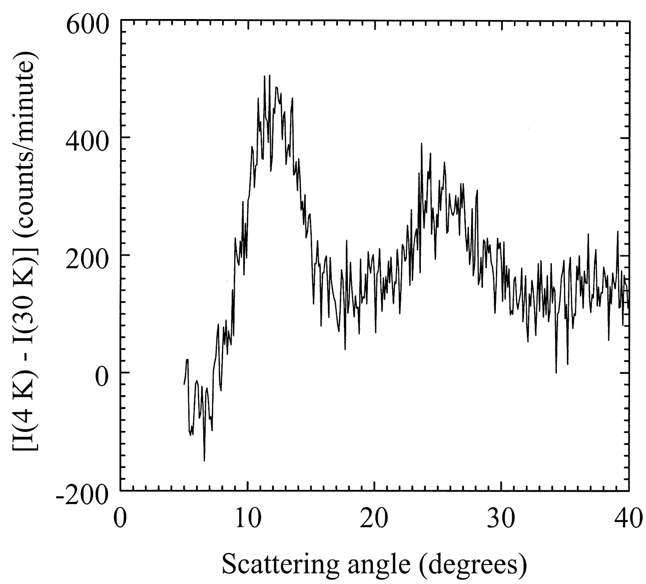

Fig. 2. Powder neutron diffraction data taken for crushed single grains of icosahedral Tb–Mg–Zn. The difference intensity (I) was calculated from $[I(4\text{ K}) - I(30\text{ K})]$. From Islam et al. [9].

temperature spin glass state are clearly evident from the slowly varying intensity shown in Fig. 2. This low-temperature spin-glass state is best characterized by thermodynamic measurements, as described previously [12], and summarized below.

The magnetization of the magnetic rare earth containing R–Mg–Zn quasicrystals is isotropic for temperatures greater than T_f (see inset to Fig. 3(a)). The susceptibility follows a Curie Weiss temperature dependence with the full theoretical effective moment derived from the Hund's rule J-multiplet, with only small deviations a few Kelvin above T_f (Fig. 3(a)). The Weiss temperatures are all negative, implying predominantly antiferromagnetic interactions between the rare earth ions. The small deviations from Curie Weiss law a few Kelvin above T_f are associated with antiferromagnetic clusters, presumably related to the short range correlations observed by Sato et al. [10] in Ho–Mg–Zn for temperatures a few Kelvin greater than T_f. These deviations are very small compared to many canonical spin glasses (see, for instance, Ref. [15]), for which cluster glass behaviour can be a pervasive problem, due to the underlying crystallinity of the non-magnetic host. In fact, the lack of an underlying tendency towards crystallinity in the case of quasicrystals, combined with the good local moment behaviour of the rare earths, might lead us to categorize the icosahedral R–Mg–Zn family as ''perfect'' spin glasses.

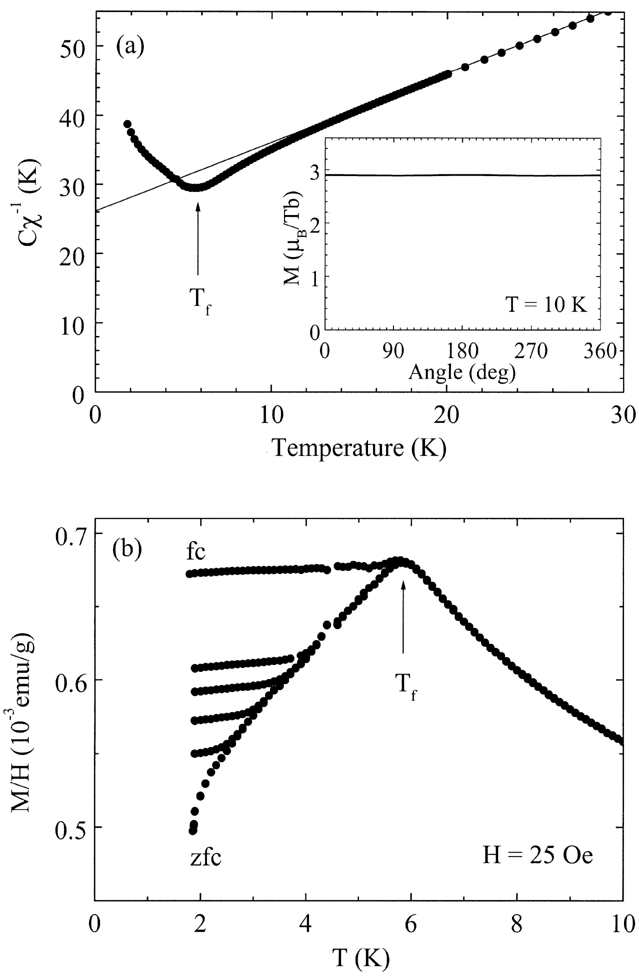

Fig. 3. (a) The inverse susceptibility of Tb–Mg–Zn, measured in an applied field of 1 kOe. The data have been normalized by the experimentally determined Curie constant C, such that the y-intercept$=\theta$. Line shows extrapolation of high-temperature fit to Curie Weiss law. Inset shows the angular dependence of the dc magnetization of Tb–Mg–Zn at 10 K (i.e. $T>T_f$) and in an applied field of 55 kOe. (b) The temperature dependence of the dc magnetization of Tb–Mg–Zn in an applied field of 25 Oe, following an initial zero-field-cool or field-cool (labeled in figure). Additional data taken following a field-cool from temperatures less than T_f (from 2.5, 3.0, 3.5 and 4.0 K) are also shown. After Fisher et al. [12].

The spin freezing transition is characterized by a sharp feature in the dc magnetization with a pronounced difference between zfc and fc data, even for very small applied fields. We have been able to identify this sharp feature in the dc magnetization with a spin freezing phenomenon because of the observation of a sharp peak in the non-linear ac susceptibility [12]. Typical dc magnetization data for Tb–Mg–Zn are shown in Fig. 3(b), taken in an applied field of 25 Oe. The freezing temperature (5.8 K) is given by the maximum in the zfc magnetization data. Additional data shown in Fig. 3(b) were taken after field-cooling from four intermediate temperatures less than T_f, illustrating the many metastable states below the freezing transition. In addition to the dc magnetization data, the frequency-dependence of the ac susceptibility has allowed us to classify the icosahedral R–Mg–Zn quasicrystals as spin glasses with a moderate strength RKKY interaction between the magnetic moments [12].

In order to investigate the effect of the local crystal electric field (CEF) of the rare earth ions on the freezing transition, the magnetic properties of the solid solutions $(Y_{1-x}Tb_x)$–Mg–Zn ($x=0.075$, 0.15, 0.33, 0.50, 0.63, 0.75 and 0.88) and $(Y_{1-x}Gd_x)$–Mg–Zn ($x=0.075$, 0.15, 0.50 and 0.60) were measured. With a half-filled 4f shell, Gd is insensitive to CEF effects, whereas the Hund's rule J-multiplet of Tb can be split by the local CEF environment. These magnetization data are discussed in more detail in Ref. [12], and are summarized in Fig. 4. The Weiss temperatures (θ) of the samples, estimated from linear fits to the inverse susceptibility, scale with the de Gennes factor $[dG=(g-1)^2J(J+1)]$ of the rare earths, indicating that θ is a good measure of the strength of the exchange interaction for both series of solid solutions, and also for the pure compounds (Fig. 4(a)). However, the freezing temperature (from the peak in the dc susceptibility) is significantly lower for the $(Y_{1-x}Gd_x)$–Mg–Zn solid solution than the other compounds for the same strength of the exchange interaction (Fig. 4(b and c)). The factor of two difference between the Heisenberg-like $(Y_{1-x}Gd_x)$–Mg–Zn series and the other moment bearing rare earths (Fig. 4) is close to the factor of 3 previously observed between Heisenberg and Ising spin glass systems [16]. These data are clear evidence that both the local rare

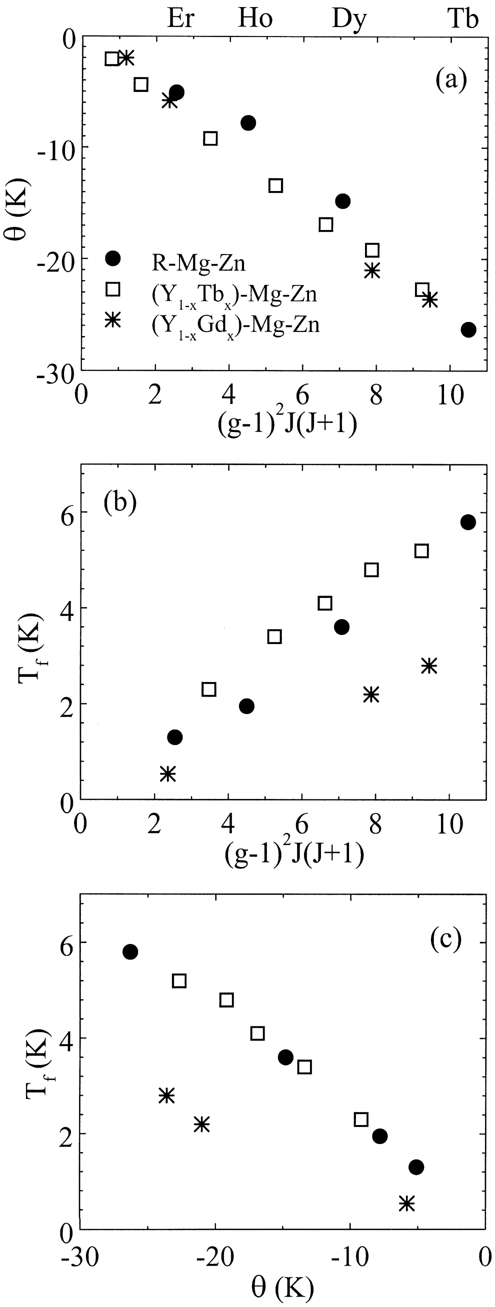

Fig. 4. The Weiss temperature (a) and the spin freezing temperature (b) vs. the de Gennes factor for R–Mg–Zn (solid circles: R = Tb, Dy, Ho and Er), $(Y_{1-x}Tb_x)$–Mg–Zn (open squares) and $(Y_{1-x}Gd_x)$–Mg–Zn (stars). Lower panel (c) shows the spin freezing temperature vs. the Weiss temperature for the same compounds. Elemental symbols along the top of (a) indicate the de Gennes factor for the ternary R–Mg–Zn compounds. From Fisher et al. [12].

earth environment and the multiplicity of R–R distances in the quasicrystal lattice contribute to T_f.

To further investigate the effects of crystal field splitting on the freezing temperature, the two magnetic rare earth substitutions $(Tb_{0.75}R_{0.25})$–Mg–Zn and $(Dy_{0.8}R'_{0.2})$–Mg–Zn were also prepared, where R and R′ = Gd, Tb, Dy, Ho

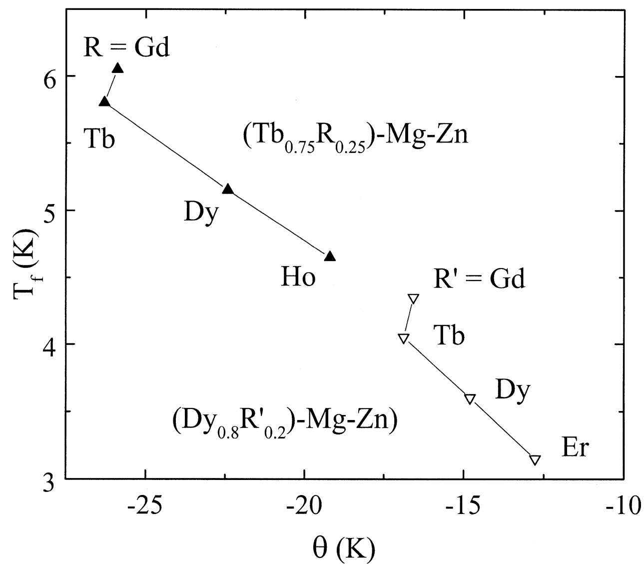

Fig. 5. The freezing temperature as a function of the Weiss temperature of the two magnetic rare earth substitutions $(Tb_{0.75}R_{0.25})$–Mg–Zn (solid up triangles) and $(Dy_{0.8}R'_{0.2})$–Mg–Zn (open down triangles), where R and R′ are annotated in the figure. Lines are drawn to guide the eye, following the de Gennes factor of the substituting ion.

and Er. Preliminary data for both of the dilution series are summarized in Fig. 5, showing the freezing temperature (as determined from the peak in the dc magnetization) as a function of the Weiss temperature θ (extracted from the high-temperature ($T > 30$ K) fit to $\chi^{-1}(T)$). Similar to previous dilution series discussed above, the freezing temperatures of the non-Heisenberg moments (Tb, Dy, Ho and Er) diluted into Tb–Mg–Zn and Dy–Mg–Zn appear to scale monotonically with the Weiss temperature, and indeed fall onto the general manifold shown in Fig. 4(c). However, the two Gd dilutions lie off this manifold and, for that matter, also lie off the equivalent de Gennes plot of Fig. 4(a). That is to say that, the Gd dilutions $(Tb_{0.75}Gd_{0.25})$–Mg–Zn and $(Dy_{0.8}Gd_{0.2})$–Mg–Zn shown in Fig. 5 have unexpectedly low θ values, but T_f values that appear to scale with the de Gennes factor.

Although the non-de Gennes scaling of θ for Gd substitutions in Tb–Mg–Zn and Dy–Mg–Zn is poorly understood, the empirical statement remains, that T_f is greater for the Gd substituted Tb–Mg–Zn than the pure Tb–Mg–Zn compound (and likewise comparing Gd and Tb substitutions in Dy–Mg–Zn). For these relatively small concentrations of Gd ($x = 0.2$ and 0.25), it is likely that T_f of $(Tb_{1-x}Gd_x)$–Mg–Zn is increased by the larger value of the average de Gennes factor for the system, and indeed the freezing temperatures scale reasonably well with the average de Gennes factor $((1-x)\times dG(Tb) + x\times dG(Gd))$. However, T_f of pure Gd–Mg–Zn (approximately 5 K, as determined from the peak in the dc magnetization of samples prepared by a rapid cooling technique [4], and consistent with our $(Y_{1-x}Gd_x)$–Mg–Zn data [12]), is *less* than that of pure Tb–Mg–Zn (5.8 K). Hence, we anticipate that large values of x in the dilution series ($Tb_{1-x}Gd_x$)–Mg–Zn must eventually *suppress* T_f. That is to say, that we predict that for the series ($Tb_{1-x}Gd_x$)–Mg–Zn there is a *maximum* value of T_f at a particular concentration (some kind of a percolation threshold). Addition of further Gd beyond this cross-over value should actually reduce T_f of ($Tb_{1-x}Gd_x$)–Mg–Zn, despite the increased de Gennes factor. The mechanism of the suppression of T_f for large Gd concentrations is likely the same as that which results in a lower value of T_f for ($Y_{1-x}Gd_x$)–Mg–Zn than that observed for ($Y_{1-x}Tb_x$)–Mg–Zn (as shown in Fig. 4): namely the isotropic nature of the Gd (Heisenberg) moments as opposed to the non-Heisenberg nature of the Tb and Dy host systems. These most recent results are currently being extended to fully understand the role of the substitution of Heisenberg and non-Heisenberg moments in the R–Mg–Zn spin glasses.

4. Conclusions

Using high-quality, single-grain samples [8], we have shown that there is no long range magnetic order in the icosahedral R–Mg–Zn quasicrystals [9], contradicting earlier preliminary measurements using polygrain (multiphase) samples [6]. We have unambiguously demonstrated the spin-glass nature of the low-temperature state via thermodynamic measurements [12]. Furthermore, by consideration of the Heisenberg spin glass ($Y_{1-x}Gd_x$)–Mg–Zn and the non-Heisenberg system ($Y_{1-x}Tb_x$)–Mg–Zn, we have shown that both the local rare earth environment and the multiplicity of R–R distances in the quasicrystal lattice contribute to T_f. The observation of an isotropic magnetization for temperatures greater than T_f does not preclude these CEF effects, but rather suggests that the observed magnetization is an average over many different rare earth sites. Further evidence for the differences between Heisenberg and non-Heisenberg moments in these spin glasses are found in the magnetic rare earth substitutions ($Tb_{1-x}R_{1-x}$)–Mg–Zn and ($Dy_{1-x}R'_{1-x}$)–Mg–Zn.

Acknowledgements

We would like to thank A.N. Hvitved, A.F. Panchula, M.J. Sailer and J. Schissel for help in sample preparation. Ames Laboratory is operated for the US Department of Energy under Contract No. W-7405-Eng-82. This work was supported by the Director for Energy Research, Office of Basic Energy Sciences.

References

[1] For instance, C. Janot, in: Quasicrystals, a primer. Clarendon Press, Oxford, 1992.
[2] Z. Luo, S. Zhang, Y. Tang, D. Zhau, Scr. Metall. Mat. 28 (1993) 1513.
[3] A.P. Tsai, A. Niikura, A. Inoue, T. Masumoto, Y. Nishida, K. Tsuda, M. Tanaka, Phil. Mag. Lett. 70 (1994) 169.
[4] Y. Hattori, A. Niikura, A.P. Tsai, A. Inoue, T. Masumoto, K. Fukamichi, H. Aruga-Katori, T. Goto, J. Phys. Condens. Matter 7 (1995) 2313.
[5] B. Charrier, D. Schmitt, J. Magn. Magn. Mat. 171 (1997) 106.
[6] B. Charrier, B. Ouladdiaf, D. Schmitt, Phys. Rev. Lett. 78 (1997) 4637.
[7] R. Lifshitz, Phys. Rev. Lett. 80 (1998) 2717.
[8] I.R. Fisher, Z. Islam, A.F. Panchula, K.O. Cheon, M.J. Kramer, P.C. Canfield, A.I. Goldman, Phil. Mag. B 77 (1998) 1601.
[9] Z. Islam, I.R. Fisher, J. Zarestky, P.C. Canfield, C. Stassis, A.I. Goldman, Phys. Rev. B 57 (1998) 11047.
[10] T.J. Sato, H. Takakura, A.P. Tsai, K. Shibata, Phys. Rev. Lett. 81 (1998) 2364.
[11] I.R. Fisher, M.J. Kramer, Z. Islam, T.A. Wiener, A. Kracher, A.R. Ross, T.A. Lograsso, A.I. Goldman, P.C. Canfield, to be published in: Proc. 7th International Conference on Quasicrystals, Stuttgart, 1999.
[12] I.R. Fisher, K.O. Cheon, A.F. Panchula, P.C. Canfield, M. Chernikov, H.R. Ott, K. Dennis, Phys. Rev. B 59 (1999) 308.
[13] A. Langsdorf, F. Ritter, W. Assmus, Phil. Mag. Lett. 75 (1997) 381.
[14] I.R. Fisher, M.J. Kramer, Z. Islam, A.R. Ross, A. Kracher, T. Wiener, M.J. Sailer, A.I. Goldman, P.C. Canfield, Phil. Mag. B 79 (1999) 425.
[15] J.A. Mydosh, in: Spin Glasses: an Experimental Introduction, Taylor and Francis, London, 1993.
[16] K. Baberschke, P. Pureur, A. Fert, R. Wendler, S. Senoussi, Phys. Rev. B 29 (1984) 4999.